Real-Time RMS-EMT Co-Simulation and Its Application in HIL Testing of Protective Relays

Renzo G. Fabián Espinoza, Guilherme Justino, Rodrigo B. Otto and Rodrigo Ramos

***Abstract*—This work proposes an interfacing technique that uses the built-in three-phase transmission line models available in simulation platforms to perform Root Mean Square (RMS)-Electromagnetic Transient (EMT) real-time, multi-domain and multi-rate co-simulation. The main objective of this paper is to show the application of this kind of simulation in hardware-in-the-loop (HIL) testing of protective relays. Two well-known platforms are considered in this work: OPAL-RT with its ePhasorSim tool is used for RMS simulation, and RTDS is used for EMT simulation. However, the proposed technique is sufficiently general to be applied to other real-time simulation platforms that have similar built-in transmission line models. To convert waveforms to phasors, a non-buffered rapid curve fitting method was implemented to attend to real-time constraints. During the testing phase of this research, tests for the HIL were completed using an actual transmission line protection relay. The presented results of tests highlight the benefits of the proposed interfacing technique.**

***Keywords*—Real-time simulation, co-simulation, hardware-in-the-loop, protective relay, multi-domain, multi-rate.**

I. Introduction

THE computational process involved in real-time simulations requires calculations to be finished before the end of each time step. Therefore, the size of the modeled electrical system is limited to enable the real-time simulation. In the case of Electromagnetic Transient (EMT) approach to conduct Hardware-in-the-Loop (HIL) tests by means of digital real-time simulation, usually the electrical system to be studied is reduced considering this limitation, using Thevenin equivalents. This practice is common in HIL protective relay tests. This reduction eliminates the dynamics of the reduced part and, thus, a co-simulation multi-domain approach is interesting because it maintains the EMT details of the studied circuit and the dynamics of the external circuit.

There is increasing interest among utilities in performing real-time simulations of large power systems. If a large power system is simulated using EMT real-time simulators, the cost of hardware can be restricting to many users. There have been many efforts to develop real-time multi-domain co-simulation platforms where the portion of the network that needs to be modeled with details is done so using EMT models, while the remaining part is modeled using Root Mean Square (RMS) models [1]–[15]. A vast review of advanced laboratory technique methods that include co-simulation frameworks is presented in [16].

This work proposes a transmission line interfacing technique that uses the built-in transmission line models available on real-time simulators to conduct real-time, multi-domain, and multi-rate co-simulation using OPAL-RT and RTDS platforms. The ePhasorSim [17] tool of OPAL-RT is used as the RMS simulator, and RTDS is used as the EMT simulator. The analog inputs and outputs of both simulators are used as communication interface. RTDS is an EMT-focused simulator that requires detailed modeling and time steps on the order of microseconds; on the other hand, ePhasorSim allows the RMS simulation and can run using time steps on the order of milliseconds. Therefore, it is possible to conduct a detailed EMT simulation interacting with an RMS simulation that allows the user to expand the studied electrical system and explore the benefits of both approaches. The main purpose of this work is to allow RMS-EMT real-time HIL tests of protective relays having the external electrical power system in an RMS solution and the electrical system of interest in an EMT solution. The EMT part interacts directly with the protective relay under test.

The remainder of this paper is structured as follows. In section II, the proposed technique is described. In section III, the results of tests considering two transmission systems of four and five buses are analyzed, as well as HIL tests using a real protective relay. Finally, section IV presents the main conclusions of this work and address future directions for research.

II. The Proposed Transmission Line Interface

The proposed interface is suitable to decouple large systems, which is suitable for parallel computation because the transmission line can be expressed as separated resistive Norton or Thevenin circuits from either side using information from previous time steps [18]. Some works, such as [19]–[21], show advanced techniques to implement a transmission line interface between RMS and EMT simulations. These methods were developed to be used in offline simulation, and most of them should be adapted to be used in real-time simulation. As described in [22], Bergeron's model and its principle implementation is used as a base principle for many methods, and they consider half of the line in the RMS domain and the other half in the EMT domain. Specifically, for RMS-EMT real-time co-simulation, [7], [15] uses a hybrid transmission

Renzo Fabián Espinoza, Guilherme Justino and Rodrigo Otto are with Center of Automation and Simulation of Electrical Systems at Itaipu Technological Park Foundation, Foz do Iguaçu, PR, Brazil; e-mail: renzo.esinoza@pti.org.br, guilherme.justino@pti.org.br, rodrigobueno@pti.org.br.

Rodrigo Ramos is with the São Carlos School of Engineering, University of Sao Paulo, SP, Brazil. e-mail: rodrigo.ramos@ieee.org

Paper submitted to the International Conference on Power Systems Transients (IPST2021) in Belo Horizonte, Brazil June 17-20, 2021.

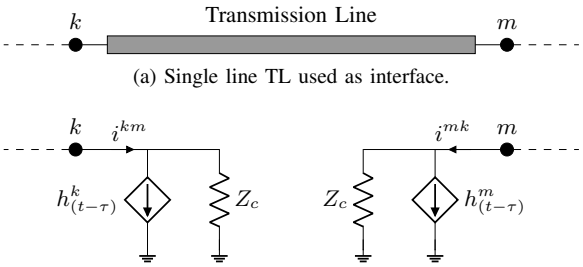

(a) Single line TL used as interface.

(b) Bergeron model used by EMT simulators.

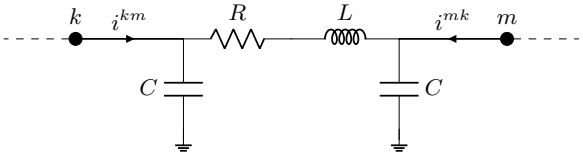

(c) Lumped parameters used by Phasor solution.

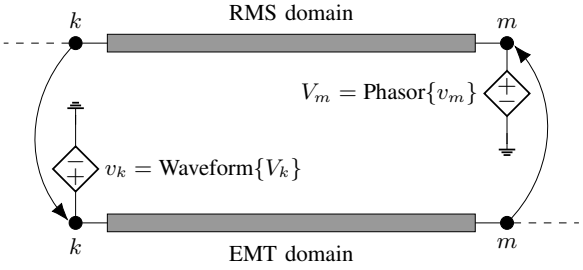

(d) Transmission line interface from RMS to EMT domain.

Figure 1. Proposed transmission line interface.

line as the RMS-EMT interface. The implementation of this approach requires programming the transmission line model in the respective tool that is available in any real-time simulator. This task is not trivial considering a three-phase coupled lossy transmission line, even though there are methods to divide the transmission into some lossless parts and place the losses at the ends of these parts. It should be noted that all methods require any kind of conversion waveform-phasor and phasor-waveform. In this work, the use of built-in transmission line components from OPAL-RT (RMS) and RTDS (EMT) are utilized, and the conversion waveform-phasor and phasor-waveform are implemented.

Figure 1 serves to explain the main idea of the proposed method, where k is the terminal of the RMS side and m is the terminal of the EMT side. The transmission line of Figure 1a is the interface of both domains (RMS and EMT). Figure 1b shows a simplified single phase lossless model of the transmission line used by EMT solution (RTDS in this case). It is the Bergeron model of transmission line [22], where,

$$i^{km}_{(t)} = \frac{v^k_{(t)}}{Z_c} + h^k_{(t-\tau)}\,; \quad (1)$$

$$i^{mk}_{(t)} = \frac{v^m_{(t)}}{Z_c} + h^m_{(t-\tau)}\,; \quad (2)$$

$$h^k_{(t-\tau)} = -\frac{v^m_{(t-\tau)}}{Z_c} - i^{mk}_{(t-\tau)}\,; \quad (3)$$

$$h^m_{(t-\tau)} = -\frac{v^k_{(t-\tau)}}{Z_c} - i^{km}_{(t-\tau)}\,. \quad (4)$$

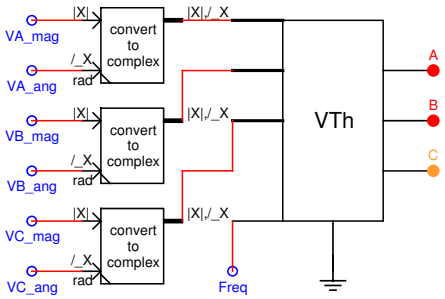

Figure 2. Three-phase controlled voltage source developed in C language by means of Cbuilder tool from RTDS.

From Eqs. (1) to (4), it is possible to observe that the controlled current source of one side only depends on the voltage of the other terminal at previous time-steps. Thus, this work proposes to impose the voltage on the RMS side (k) using the transmission line model available in RTDS, instead of implementing the controlled source $h^m_{(t-\tau)}$. Figure 1c shows a single-phase transmission line model used by ePhasorSim.

It is possible to see that if the voltage at m is known, the RMS side simulation can be conducted. Figure 1d shows the interface that is used by both simulators.

In this implementation, the k voltage of the RMS side is converted to an EMT waveform and injected into the EMT simulator with a controlled voltage source. This is accomplished in such a way that the m voltage of the EMT side is converted to RMS phasors and injected into the RMS simulator using a voltage source.

A. Phasor to EMT conversion

The following equations are used to convert the phasors to EMT waveforms:

$$v_a(t) = \sqrt{2}\,\mathrm{Re}\{V_a(t)\}\cos(wt) - \sqrt{2}\,\mathrm{Im}\{V_a(t)\}\sin(wt)\,; \quad (5)$$

$$v_b(t) = \sqrt{2}\,\mathrm{Re}\{V_b(t)\}\cos(wt) - \sqrt{2}\,\mathrm{Im}\{V_b(t)\}\sin(wt)\,; \quad (6)$$

$$v_c(t) = \sqrt{2}\,\mathrm{Re}\{V_c(t)\}\cos(wt) - \sqrt{2}\,\mathrm{Im}\{V_c(t)\}\sin(wt)\,. \quad (7)$$

Where $V_a(t)$, $V_b(t)$ and $V_c(t)$ are the voltage phasors at instant t and $w = 2\pi f(t)$ is the phasor frequency, considering that in the more general case, f is time dependent also. A controlled voltage source component was implemented in C language using the RTDS CBuilder tool as shown in Figure 2, because there is no built-in voltage source capable of generating the corresponding waveform with this flexibility available in RTDS. This three-phase controlled voltage source was implemented with its Norton equivalents because RTDS uses Norton sources for implementing electrical components. A minimum series resistance for the Thevenin equivalent was considered. It has the three magnitudes and angles, as well as the desired frequency, as inputs at which waveforms are generated.

B. EMT to phasor conversion

Fourier-based and curve fitting (CF) methods are two widely used approaches to convert time-domain quantities to their frequency-domain counterparts. Fourier-based methods have a sampling rate and amount of processed samples constraints

related to the fundamental frequency to obtain its correct phasor representation. Thus, they have a delay associated with the amount of processed samples, and this may cause inaccuracies in the overall simulation. This constraint is notorious in this kind of application because in real-time simulation, a rapid response is necessary because the calculated variables will be sent to the other part of the co-simulation.

In the proposed method, the phasors are exchanged between the two simulators. In the protection relay testing application, the waveforms of voltage and current are sent from the real-time simulator to the device under test (DUT) and binary variables are exchanges between the real-time simulator and the DUT. Thus there is an strong interaction between the real-time simulators because the stability of the co-simulation depends on the velocity and precision of the exchanged data. On the other hand, CF methods are computationally less expensive and render more flexibility in the sampling requirements. CF methods can also be applied with few samples [23], but they lose accuracy when the signal presents any DC offset. In this sense, an advantage of the proposed method is the fact that it only uses the exchange of voltages between the real-time simulators, considering that voltage has more stable behavior than current.

According to [24], the phasor can be calculated using CF approach by

$$\begin{bmatrix} \mathrm{Re}\{V\} \\ -\mathrm{Im}\{V\} \end{bmatrix} = inv(\mathbf{F}' \times \mathbf{F}) \times (\mathbf{F}' \times \mathbf{v})\,. \tag{8}$$

Where,

$$\mathbf{v} = \begin{bmatrix} v(t_1) \\ \vdots \\ v(t_N) \end{bmatrix}, \quad \mathbf{F} = \begin{bmatrix} \cos(wt_1) & \sin(wt_1) \\ \vdots & \vdots \\ \cos(wt_N) & \sin(wt_N) \end{bmatrix}.$$

Where N is the number of samples, $\mathbf{v}$ is a vector of samples at each time-step and $\mathbf{F}$ is the $N \times 2$ curve fitting matrix. To obtain a non-buffered algorithm, it is possible to manipulate (8) using the following relations:

$$\mathbf{F}' \times \mathbf{F} = \begin{bmatrix} \sum_{n=0}^{N} \cos^2(wt_n) & \sum_{n=0}^{N} \cos(wt_n)\sin(wt_n) \\ \sum_{n=0}^{N} \cos(wt_n)\sin(wt_n) & \sum_{n=0}^{N} \sin^2(wt_n) \end{bmatrix}; \tag{9}$$

$$a = \sum_{n=0}^{N} \cos^2(wt_n)\,; \tag{10}$$

$$b = \sum_{n=0}^{N} \cos(wt_n)\sin(wt_n)\,; \tag{11}$$

$$c = b\,; \tag{12}$$

$$d = \sum_{n=0}^{N} \sin^2(wt_n)\,; \tag{13}$$

$$inv(\mathbf{F}' \times \mathbf{F}) = \begin{bmatrix} a & b \\ b & d \end{bmatrix}^{-1}; \tag{14}$$

input : $v(t)$, t, f
output: $\mathrm{Re}\{V\}$, $\mathrm{Im}\{V\}$

$w = 2\pi f$
$a = \cos(wt)\cos(wt) + a$
$b = \cos(wt)\sin(wt) + b$
$d = \sin(wt)\sin(wt) + d$
$x = v(t)\cos(wt) + x$
$y = v(t)\sin(wt) + y$
n=n+1

if n == N **then**

Denom $= \sqrt{2}(ad - b^2)$
$A = d/\mathrm{Denom}$
$B = b/\mathrm{Denom}$
$C = -b/\mathrm{Denom}$
$D = a/\mathrm{Denom}$

$\mathrm{Re}\{V\} = A \times x + B \times y$
$\mathrm{Im}\{V\} = -C \times x - D \times y$

$n = 0$, $a = 0$, $b = 0$, $d = 0$, $x = 0$, $y = 0$

Figure 3. Non-buffered distributed curve fitting algorithm that is executed at each time-step. at RTDS.

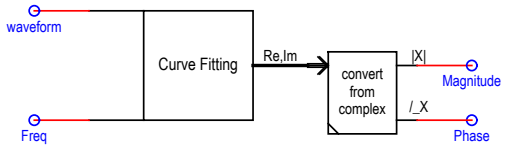

Figure 4. Curve fitting phasor calculator developed in C language by means of Cbuilder tool from RTDS.

$$inv(\mathbf{F}' \times \mathbf{F}) = \begin{bmatrix} A = \dfrac{d}{ad - b^2} & B = \dfrac{b}{ad - b^2} \\ C = \dfrac{-b}{ad - b^2} & D = \dfrac{a}{ad - b^2} \end{bmatrix}; \tag{15}$$

$$\mathbf{F}' \times \mathbf{v} = \begin{bmatrix} x = \sum_{n=0}^{N} \cos(wt_n)v(t_n) \\ y = \sum_{n=0}^{N} \sin(wt_n)v(t_n) \end{bmatrix}; \tag{16}$$

$$\begin{bmatrix} \mathrm{Re}\{V\} \\ -\mathrm{Im}\{V\} \end{bmatrix} = \begin{bmatrix} A & B \\ C & D \end{bmatrix} \times \begin{bmatrix} x \\ y \end{bmatrix}. \tag{17}$$

It was implemented by distributing the computation process at each time-step of the simulation and without using buffers which save the samples, in order to be executed in real-time without overruns. The derived algorithm is shown Figure 3. Additionally, a sliding window was implemented to obtain a smooth phasor updating.

The CF component was implemented by means of CBuilber tool of RTDS to extract the voltage phasors at the m terminal based on (9)-(17). This component is shown in Figure 4 and has as input the signal waveform values and the frequency at which the phasor will be calculated.

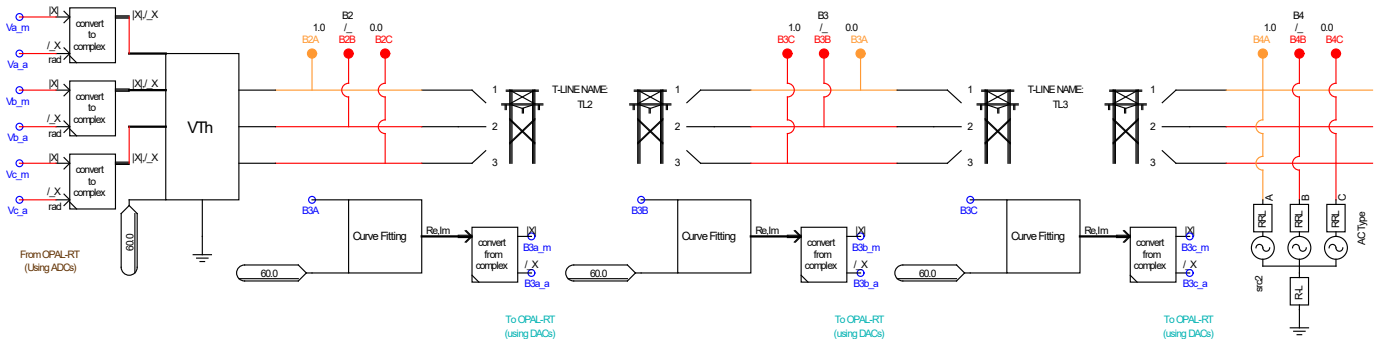

Figure 5. RSCAD implementation of the co-simulation case for the electrical system of Figure 6a, which has a voltage source on the EMT side

.

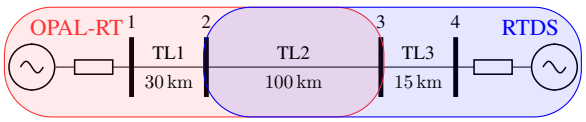

S1: $1.0\angle 0$ p.u.
$Z_0 = (8.317 + \mathrm{j}30.116)\,\Omega$
$Z_1 = (2.548 + \mathrm{j}12.271)\,\Omega$

S2: $0.96\angle 11.3°$ p.u.
$Z_0 = (8.317 + \mathrm{j}30.116)\,\Omega$
$Z_1 = (2.548 + \mathrm{j}12.271)\,\Omega$

TL1, TL2, TL3:
$Z'_0 = (0.3616 + \mathrm{j}1.3094)\,\Omega\,\mathrm{km}^{-1}$ $Y'_0 = 2.234\,\mu\mathrm{S}\,\mathrm{km}^{-1}$
$Z'_1 = (0.1108 + \mathrm{j}0.5335)\,\Omega\,\mathrm{km}^{-1}$ $Y'_1 = 3.104\,\mu\mathrm{S}\,\mathrm{km}^{-1}$

(a) Electrical system with a voltage source in the EMT side.

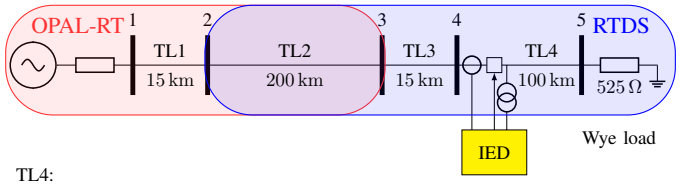

TL4:
$Z'_0 = (0.3618 + \mathrm{j}1.2277)\,\Omega\,\mathrm{km}^{-1}$ $Y'_0 = 2.8975\,\mu\mathrm{S}\,\mathrm{km}^{-1}$
$Z'_1 = (0.0185 + \mathrm{j}0.3766)\,\Omega\,\mathrm{km}^{-1}$ $Y'_1 = 4.3881\,\mu\mathrm{S}\,\mathrm{km}^{-1}$

(b) Electrical system for HIL tests.

Figure 6. Electrical systems of 230 kV used in the simulations.

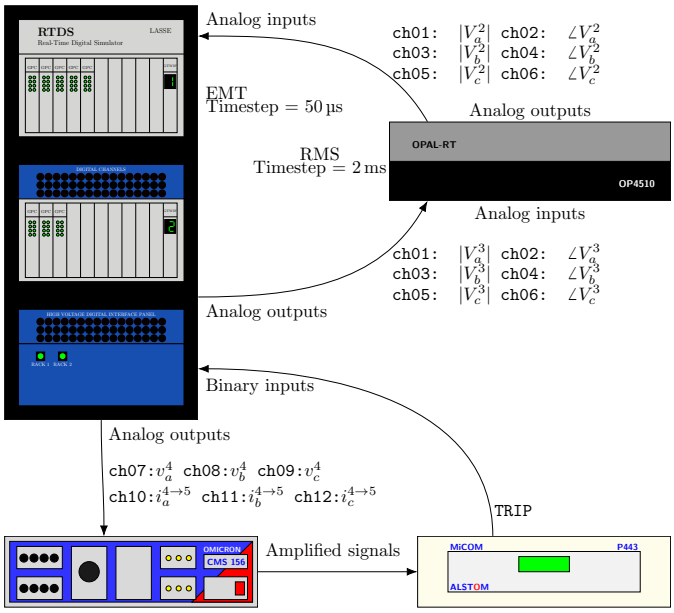

Figure 7. Co-simulation HIL setup using RTDS and OPAL-RT simulators, considering voltage and current amplifier and a protective relay.

III. Test and Results

Figure 5 shows the RSCAD model implementation of the co-simulation case corresponding to the electrical system of Figure 6a. It is worth noting the three-phase controlled voltage source is used at a fixed frequency 60 Hz because ePhasorSim in three-phase solution mode does not consider variations in frequency. Frequency variations are considered only in the positive sequence solution mode. The voltage phasors are received into RTDS from the ePhasorSim solution. There are the three CF components on Figure 5 that convert the voltage waveforms of Bus 3 to phasors that are then sent to the ePhasorSim. In this case, the frequency is fixed to 60 Hz as well. If frequency is considered time varying due to generator dynamics, this value will be provided by the RMS simulation and must be sent to the EMT side. It will be used as input in the controlled voltage source and CF components.

The electrical systems shown in Figure 6 were used to test the proposed method, where TL2 was used as the interface. This line is simulated at RMS side as well as at EMT side. The voltage (magnitude and angle) of each phase at Bus 2 provided by the ePhasorSim (OPAL-RT) simulation is sent to RTDS via six properly scaled analog outputs. These signals are received by the analog inputs of the RTDS and included in the simulation using the voltage source detailed in section II-A. The three voltages waveforms at Bus 3 are converted to phasors using the component described in section II-B at RTDS side, and the corresponding phasors are sent to the OPAL-RT with properly scaled analog outputs. The ePhasorSim solver receives the signals by the analog inputs, including them in the simulation.

Figure 7 shows the hardware configuration for the for the tests. The interaction between the real-time simulators is shown in the top part of this figure. This process is conducted asynchronously because there is no synchronization signal between the simulators. They are synchronized to the real-time clock reference by means of their internal clocks. For the tests RTDS used a 50 µs time-step with $N = 20$ for the CF algorithm, and ePhasorSim used 2 ms time steps. The digital-to-analog converters (DAC) and the analog-to-digital converters

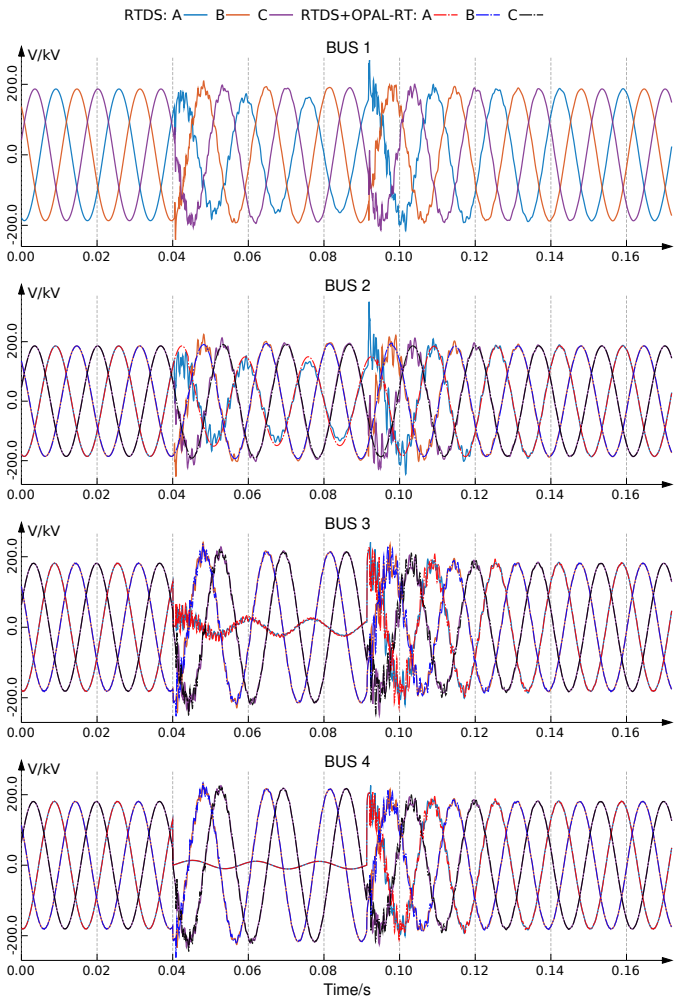

Figure 8. Voltage at buses 1, 2, 3 and 4 for the electrical system of Figure 6a and AG fault with $R_f = 1\,\Omega$.

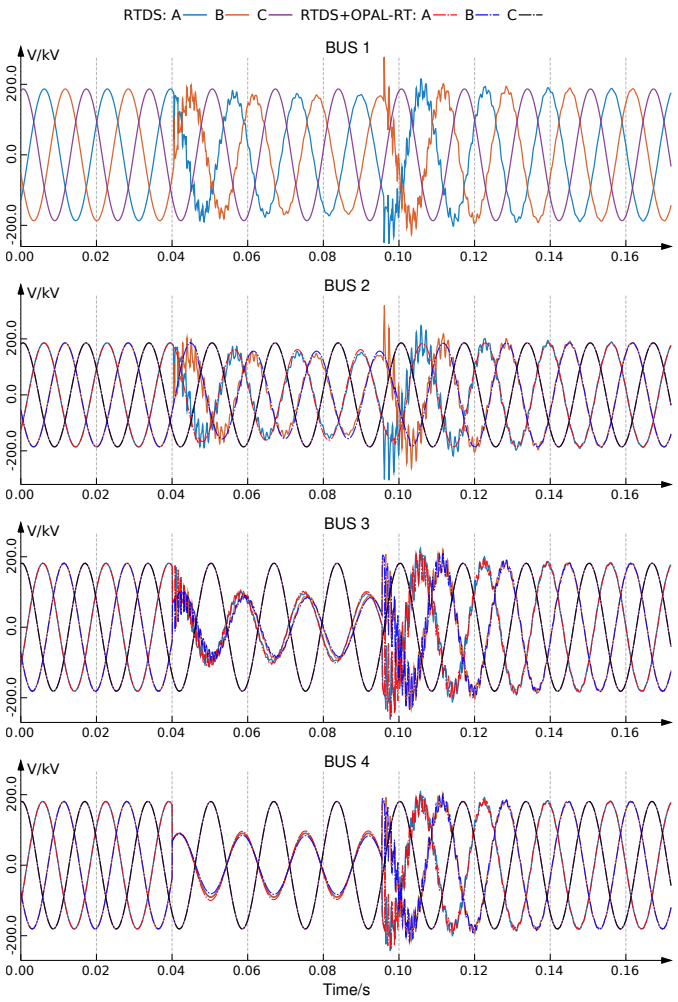

Figure 9. Voltage at buses 1, 2, 3 and 4 for the electrical system of Figure 6a and AB fault with $R_f = 1\,\Omega$.

(ADC) of RTDS and OPAL-RT have $1\,\mu s$ of conversion time, accumulating $2\,\mu s$ to arrive from one simulation to the other. Considering that the co-simulation update time is $2\,ms$, it is possible to affirm that the associated delay is not significant. On the other hand, $2\,ms >> 50\,\mu s$ and it should be noted that the waveforms only exist on the RTDS side. Furthermore, the proper voltage waveforms are generated via the controlled voltage source component by considering the time of the simulation at each time step, so it is compatible with additional sources on the RTDS side. Thus, additional synchronization, including time-step start synchronization, is not necessary as opposed to the case where EMT-EMT simulation is performed. Additionally, by using this technique it is not necessary for both simulations to begin at the same time. However, ensuring a matching power flow on the RMS side is required, together with a verification that the system operates under stable steady state conditions, before any dynamic response is simulated with the application of a disturbance. In the proposed method, these conditions are checked by ePhasorSim.

A. Preliminary tests

Initially, the performance of the proposed method is tested. First, the electrical system of Figure 6a that has a voltage source on the EMT side, is considered. A phase A to ground (AG) fault with $R_f = 1\,\Omega$ during three cycles was applied at Bus 4.

Additionally, the full electrical system was implemented in RTDS and simulated at the same time to the co-simulation system to be used as a basis of comparison. Figure 8 shows the voltage waveforms at buses 1, 2, 3, and 4 of the reference system (full RTDS) as well as the voltages waveforms of the co-simulation (RTDS+OPAL-RT). It should be noted that for Bus 1, there are waveforms only for the reference system because in the co-simulation, this bus does not exist on the RTDS side. Analyzing the behavior of the co-simulation, it is possible to see that, at Bus 2, the two waveforms have an excellent match considering that co-simulation waveforms at this bus are purely sinusoidal because they are generated via the three-phase controlled voltage source detailed at section II-A. Furthermore, the solutions of the co-simulation and the reference system at buses 3 and 4 are almost identical. Also considering the system of Figure 6a, a phase A to phase B (AB) fault with $R_f = 1\,\Omega$ during three cycles was applied at Bus 4. The corresponding voltage waveforms are plotted in Figure 9 and it is possible to see that there is also a good match

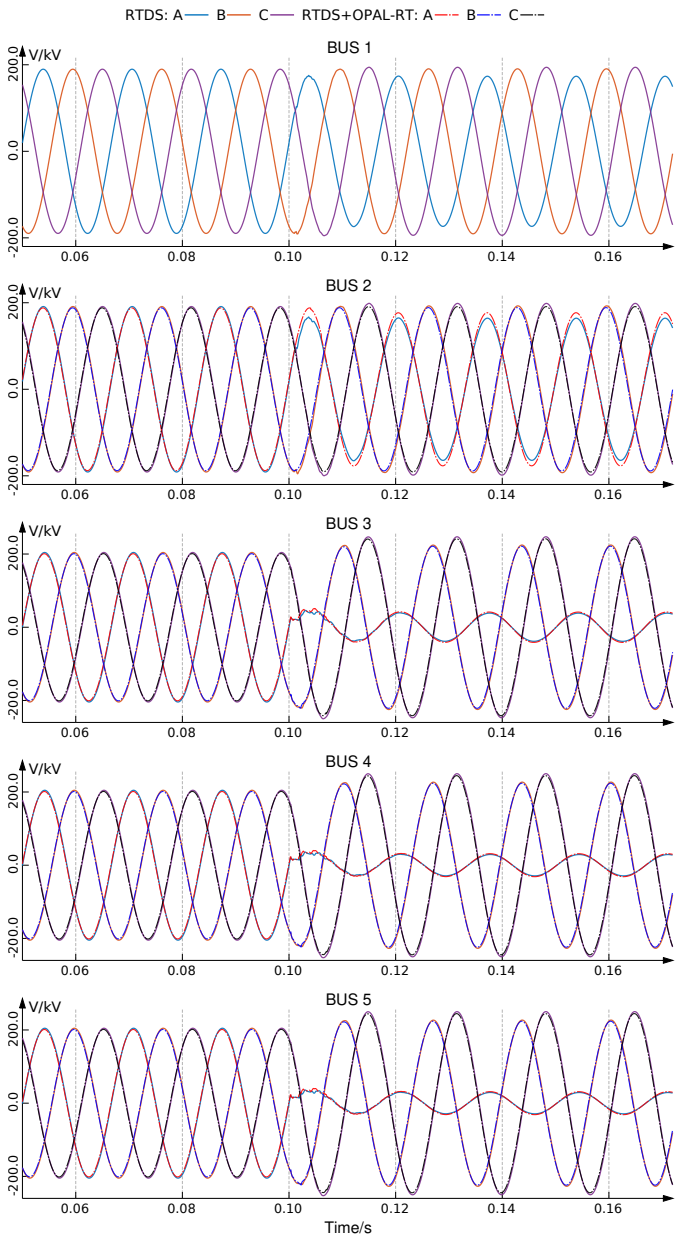

Figure 10. Voltage at buses 1, 2, 3, 4 and 5 for the electrical system of Figure 6b and AG fault with $R_f = 10\,\Omega$.

between the co-simulation and the full RTDS simulation. Additionally, the electrical system of Figure 6b without the protective relay, also known as Intelligent Electronic Device (IED), was used, where an AG fault with $R_f = 10\,\Omega$ was applied. The corresponding voltage waveforms are shown in Figure 10. It is possible to see that the proposed method works fine with voltage sources on the EMT side and without them.

B. HIL test with a protective relay

For HIL tests, the facility shown in Figure 7 is used, including a protective relay. The electrical system of Figure 6b was used for the tests. There is a protective relay (IED) at Bus 4 that monitors the TL4. The waveforms corresponding to voltages and currents at Bus 4 are generated at a low level by the RTDS with their analog outputs (DACs). These low-level signals are amplified and injected into the protective relay. This

Table I
PROTECTIVE RELAY SETTINGS FOR DISTANCE FUNCTION

Zone	Reach [%]	Time delay [s]
1	80	0
2	130	0.2

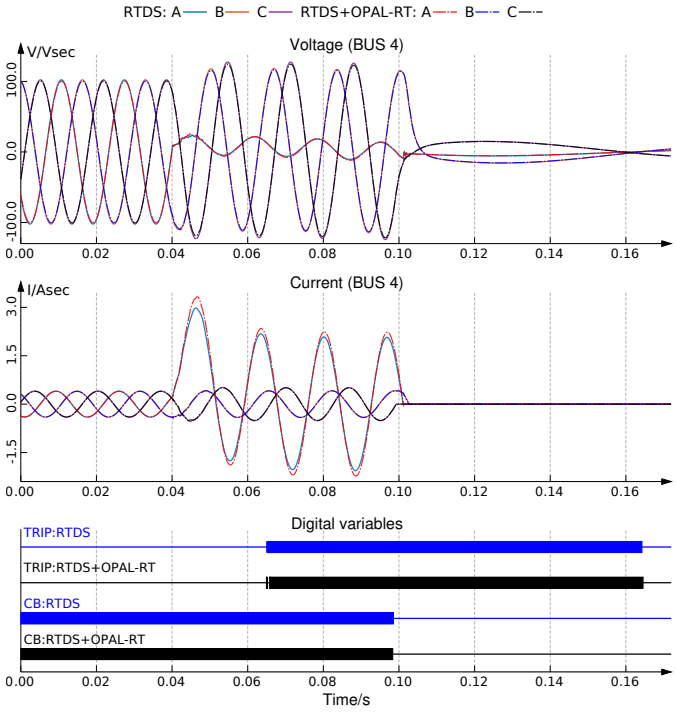

Figure 11. COMTRADE oscillographies from the protective relay for co-simulation and reference systems. AG fault at 30 km from Bus 4. $R_f = 20\,\Omega$.

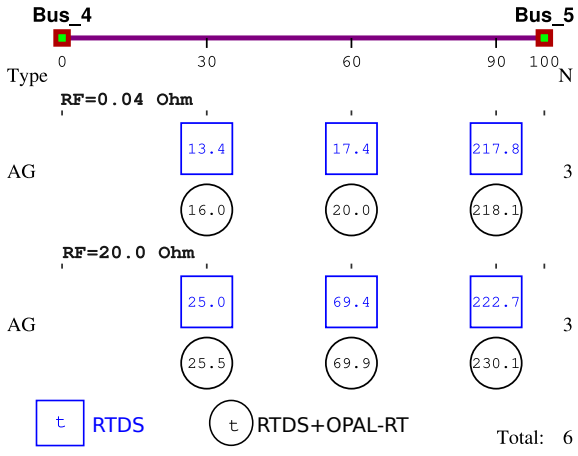

Figure 12. Protective relay operation resume.

protective relay uses the distance function with the settings shown in Table I. Figure 11 shows the COMTRADE [25] files saved by the protective relay for an AG fault that occurred at $30\,\mathrm{km}$ from Bus 4 with $R_f = 20\,\Omega$. To compare the behavior of the co-simulation, the relay response to reference and co-simulation systems are plotted simultaneously. In this figure, it is one can see that the voltage, current waveforms of the reference system, and the co-simulation are almost the same. Consequently, the relay had the same response to both events.

Figure 12 shows the protective relay response to AG faults along TL4, using the full RTDS modeled system and using the co-simulation (RTDS+OPAL-RT). The operation time is printed in milliseconds. It is possible to see that the protective relay operates similarly for both sets of tests.

IV. Conclusion

This work proposed the implementation of RMS-EMT real-time, multi-rate co-simulation using ePhasorSim tool from OPAL-RT interacting with RTDS. A transmission line was used as interface between both simulators. The built-in transmission line components of both simulators were used, avoiding the development of a hybrid RMS-EMT transmission line.

It was necessary to implement a controlled three-phase voltage source and a non-buffered CF phasor calculator using the CBuilder tool of RTDS. Considering that all methods require any kind of conversion EMT-RMS and RMS-EMT, a minimum quantity of components were developed.

The analog inputs and outputs of both simulators were used to exchange voltage phasors between the simulators. The associated delay for this application is insignificant.

The ePhasorSim in the three-phase mode was used for tests, where there are no electrical machines models available unlike the positive sequence mode, where it is possible to analyze frequency variations but negative and zero sequences are ignored; thus, only three-phase faults can be analyzed. Other Simulink packages, such as Simscape, can be used as RMS solver in OPAL-RT. Real-time simulators have a number of represented nodes' limitations. Using this co-simulation, it is possible to simulate a large number of nodes on the RMS side, allowing for changes to the topology in the circuit, switching loads and applying faults in real-time execution.

HIL tests using an actual protective relay were conducted, and the results showed that the behavior of the DUT was almost the same when the full RTDS model was used and when the co-simulation was used.

The use of digital communication interfaces is the next step of this research, which can potentially improve the precision of the proposed technique and will reduce the wiring.

Finally, the proposed method can be used by any couple of real-time simulators.

References

[1] V. Jalili-Marandi, V. Dinavahi, K. Strunz, J. A. Martinez, and A. Ramirez, "Interfacing techniques for transient stability and electromagnetic transient programs ieee task force on interfacing techniques for simulation tools," *IEEE Transactions on Power Delivery*, vol. 24, no. 4, pp. 2385–2395, 2009.

[2] V. Jalili-Marandi, F. J. Ayres, C. Dufour, and J. Bélanger, "Real-time electromagnetic and transient stability simulations for active distribution networks," 2013.

[3] Y. Liang, X. Lin, A. Gole, M. Yu, Y. Zhang, and B. Zhang, "Comparisons of impact on the modeling detail on real time simulation of large power systems with hvdc," in *IPST2011*, 2013.

[4] Yizhong Hu, Wenchuan Wu, Boming Zhang, and Qi Guo, "Development of an rtds-tsa hybrid transient simulation platform with frequency dependent network equivalents," in *IEEE PES ISGT Europe 2013*, 2013, pp. 1–5.

[5] Y. Zhang, A. M. Gole, W. Wu, B. Zhang, and H. Sun, "Development and analysis of applicability of a hybrid transient simulation platform combining tsa and emt elements," *IEEE Transactions on Power Systems*, vol. 28, no. 1, pp. 357–366, 2013.

[6] N. Panigrahy, Gopalakrishnan K. S., Ilamparithi T., and M. V. Kashinath, "Real-time phasor-emt hybrid simulation for modern power distribution grids," in *2016 IEEE International Conference on Power Electronics, Drives and Energy Systems (PEDES)*, 2016, pp. 1–6.

[7] P. Le-Huy, G. Sybille, P. Giroux, L. Loud, J. Huang, and I. Kamwa, "Real-time electromagnetic transient and transient stability co-simulation based on hybrid line modelling," *IET Generation, Transmission Distribution*, vol. 11, no. 12, pp. 2983–2990, 2017.

[8] T. Jiang, X. Song, S. Schlegel, and D. Westermann, "Hybrids-simulation using emegasim and ephasorsim for converter dominated distribution grid," in *NEIS 2018; Conference on Sustainable Energy Supply and Energy Storage Systems*, 2018, pp. 1–6.

[9] S. Vogel, V. S. Rajkumar, H. T. Nguyen, M. Stevic, R. Bhandia, K. Heussen, P. Palensky, and A. Monti, "Improvements to the co-simulation interface for geographically distributed real-time simulation," in *IECON 2019 - 45th Annual Conference of the IEEE Industrial Electronics Society*, vol. 1, Oct 2019, pp. 6655–6662.

[10] H. Konara, U. D. Annakkage, and C. Karawita, "Real-time co-simulation model using electromagnetic transient and dynamic phasor simulations," *CIGRE Science & Engineering (CSE) Journal*, 6 2019.

[11] F. Xie, C. McEntee, M. Zhang, and N. Lu, "An asynchronous real-time co-simulation platform for modeling interaction between microgrids and power distribution systems," in *2019 IEEE Power Energy Society General Meeting (PESGM)*, 2019, pp. 1–5.

[12] K. Sidwall and P. Forsyth, "Advancements in real-time simulation for the validation of grid modernization technologies," *Energies*, vol. 13, no. 16, 2020. [Online]. Available: https://www.mdpi.com/1996-1073/13/16/4036

[13] B. Li, H. Zhao, J. Diao, and M. Han, "Design of real-time co-simulation platform for wind energy conversion system," *Energy Reports*, vol. 6, pp. 403 – 409, 2020, the 6th International Conference on Power and Energy Systems Engineering. [Online]. Available: http://www.sciencedirect.com/science/article/pii/S2352484719309308

[14] J. Song, K. Hur, J. Lee, H. Lee, J. Lee, S. Jung, J. Shin, and H. Kim, "Hardware-in-the-loop simulation using real-time hybrid-simulator for dynamic performance test of power electronics equipment in large power system," *Energies*, vol. 13, no. 15, 2020. [Online]. Available: https://www.mdpi.com/1996-1073/13/15/3955

[15] P. Le-Huy, J. Huang, F. Guay, and I. Kamwa, "Hybrid simulation and off-the-shelf hardware for efficient real-time simulation studies," in *2020 6th IEEE International Energy Conference (ENERGYCon)*, 2020, pp. 98–103.

[16] J. Montoya, R. Brandl, K. Vishwanath, J. Johnson, R. Darbali-Zamora, A. Summers, J. Hashimoto, H. Kikusato, T. S. Ustun, N. Ninad, E. Apablaza-Arancibia, J.-P. Bérard, M. Rivard, S. Q. Ali, A. Obushevs, K. Heussen, R. Stanev, E. Guillo-Sansano, M. H. Syed, G. Burt, C. Cho, H.-J. Yoo, C. P. Awasthi, K. Wadhwa, and R. Bründlinger, "Advanced laboratory testing methods using real-time simulation and hardware-in-the-loop techniques: A survey of smart grid international research facility network activities," *Energies*, vol. 13, no. 12, 2020. [Online]. Available: https://www.mdpi.com/1996-1073/13/12/3267

[17] V. Jalili-Marandi, E. Robert, V. Lapointe, and J. Bélanger, "A real-time transient stability simulation tool for large-scale power systems," in *2012 IEEE Power and Energy Society General Meeting*, 2012, pp. 1–7.

[18] W. Ren, M. Steurer, and T. L. Baldwin, "Improve the stability and the accuracy of power hardware-in-the-loop simulation by selecting appropriate interface algorithms," *IEEE Transactions on Industry Applications*, vol. 44, no. 4, pp. 1286–1294, July 2008.

[19] D. Shu, X. Xie, V. Dinavahi, C. Zhang, X. Ye, and Q. Jiang, "Dynamic phasor based interface model for emt and transient stability hybrid simulations," *IEEE Transactions on Power Systems*, vol. 33, no. 4, pp. 3930–3939, 2018.

[20] K. Mudunkotuwa and S. Filizadeh, "Co-simulation of electrical networks by interfacing emt and dynamic-phasor simulators," *Electric Power Systems Research*, vol. 163, pp. 423 – 429, 2018.

[21] Y. Li, D. Shu, F. Shi, Z. Yan, Y. Zhu, and N. Tai, "A multi-rate co-simulation of combined phasor-domain and time-domain models for large-scale wind farms," *IEEE Transactions on Energy Conversion*, vol. 35, no. 1, pp. 324–335, 2020.

[22] H. W. Dommel, "Digital computer solution of electromagnetic transients in single-and multiphase networks," *IEEE Transactions on Power Apparatus and Systems*, vol. PAS-88, no. 4, pp. 388–399, 1969.

[23] T. S. Theodoro, M. A. Tomim, P. G. Barbosa, A. C. Lima, and M. T. C. de Barros], "A flexible co-simulation framework for penetration studies of power electronics based renewable sources: A new algorithm for phasor extraction," *International Journal of Electrical Power and Energy Systems*, vol. 113, pp. 419 – 435, 2019.

[24] T. S. Theodoro, M. A. Tomim, A. C. S. de Lima, and P. G. Barbosa, "A hybrid simulation tool for penetration studies of distributed generation in smartgrids," in *2017 Brazilian Power Electronics Conference (COBEP)*, 2017, pp. 1–7.

[25] "Ieee standard common format for transient data exchange (comtrade) for power systems," *IEEE Std C37.111-1999*, pp. 1–55, 1999.